off inversely with distance from an axis below the solar surface. Each of the loops is heated uniformly and viewed face-on with no assumed variation in the line of sight, so that the temperature at a given altitude on the axis of the arcade is the value at the summit of the particular loop that reaches that altitude. First, we assumed the energy is deposited uniformly per unit length, so that the heating flux is proportional to loop length, and found a very poor fit with a χ^2/n of 4.95 and a significance level below 0.1% (dotted curve in Fig. 3a). Next, we assumed instead the same heating flux on each loop and found a better (but still poor) fit with a χ^2/n of 1.83 and a significance level of 2.5% (solid curve in Fig. 3a). Finally, we considered a heating that is proportional to the square of the magnetic field strength and so decreases with altitude. This gave an excellent fit with a χ^2/n of 0.49 and a significance level of 94% (Fig. 3b).

Several different mechanisms for heating the solar corona have previously been proposed and they produce different forms of heating, so that the above result about the heating probably being distributed uniformly along large-scale diffuse loops has important implications about which mechanism is likely. In particular, we may deduce that the diffuse corona is heated locally *in situ* and rule out the previously reasonable suggestion that it is just a response to low-lying heating near the loop feet, either by the interaction of small loops that takes place in bright points or by waves of very small wavelength dumping their energy low down in the atmosphere.

Long-wavelength magnetic waves were another prime candidate for heating large coronal loops[15,16], driven resonantly by the observed solar surface motions. It has been suggested that they may dissipate and dump their energy rather non-uniformly in the coronal plasma by two mechanisms, known as phase mixing[17,18] and resonant absorption[19–21]. The fundamental standing waves (which carry the most energy) have nodes near the loop feet and their greatest amplitude near the loop summits, where the heating is therefore concentrated non-uniformly, and so such waves are unlikely to explain our observations. However, although waves seem unlikely, they cannot definitely be ruled in or out using the present technique until the spatial distribution of heating by wave mechanisms has been carefully calculated.

At present, the evidence is more in favour of another mechanism that does tend to heat the plasma uniformly, namely stochastic or turbulent dissipation in many small current sheets[22–24]. These may form in response to either the slow braiding of the magnetic footpoints in the solar surface[25,26] or local small-scale instabilities that are driven by such surface motions. In either case a state of magnetic turbulence is set up[27], which has recently been modelled in three-dimensional numerical experiments[28–30].

We have here proposed a new two-part approach to trying to solve the coronal heating problem, namely first of all to use observed temperature profiles to deduce the form of the heating in coronal loops and arcades and secondly to use that heating form to deduce the likely heating mechanism. The application of this approach here suggests that large-scale diffuse coronal loops are much more likely to be heated rather uniformly by turbulent magnetic reconnection than by preferential heating at the loop feet or loop summit. In future, it will be interesting to see whether or not the same is true for other coronal structures. In addition, it is hoped that this will act as an incentive to proponents of particular mechanisms to deduce in detail the resulting form of heating produced by their models and to observers to refine their diagnostics so as to deduce the temperature profiles with as low an error as possible. □

Received 16 May 1997; accepted 17 March 1998.

1. Ulmschneider, P., Priest, E. R. & Rosner, R. *Mechanisms of Chromospheric and Coronal Heating* (Springer, Berlin, 1991).
2. Culhane, J. L. Yohkoh observations of the solar corona. *Adv. Space Res.* **19**, 1839–1848 (1997).
3. Priest, E. R., Parnell, C. E. & Martin, S. F. A converging flux model of an x-ray bright point and an associated cancelling magnetic feature. *Astrophys. J.* **427**, 459–474 (1994).
4. Parnell, C. E., Golub, L. & Priest, E. R. The 3D structure of x-ray bright points. *Solar Phys.* **151**, 57–74 (1994).
5. Jordan, C. Modelling of solar coronal loops. *Mem. Soc. Astron. Ital.* **63**, 605–620 (1992).
6. Acton, L. W. Comparison of Yohkoh x-ray and other solar activity parameters for November 1991 to November 1995. *Astron. Soc. Pacific. Conf. Ser.* **109**, 45–54 (1996).
7. Shimizu, T., Tsuneta, S., Acton, L. W., Lemen, J. R. & Uchida, Y. Transient brightenings in active regions observed by the Yohkoh soft X-ray telescope. *Publ. Astron. Soc. Japan* **44**, L147–L153 (1992).
8. Yoshida, T. & Tsuneta, S. Temperature structure of solar active regions. *Astrophys. J.* **459**, 342–346 (1996).
9. Tsuneta, S. & Lemen, J. R. in *Physics of Solar and Stellar Coronae* 113–130 (eds Linsky, J. & Serio, S.) (Kluwer, Dordrecht, 1993).
10. Kano, R. & Tsuneta, S. Temperature distributions and energy scaling law of solar coronal loops obtained with Yohkoh. *Publ. Astron. Soc. Japan* **48**, 535–543 (1996).
11. Sturrock, P. A., Wheatland, M. S. & Acton, L. W. Yohkoh soft x-ray telescope images of the diffuse solar corona. *Astrophys. J.* **461**, L115–L117 (1996).
12. Foley, C. A., Culhane, J. L., Weston, D., Acton, L. W. & Hara, H. *Solar Phys.* (submitted).
13. Neupert, W., Nakagawa, Y. & Rust, D. M. Energy balance in a magnetically confined coronal structure observed by OSO-7. *Solar Phys.* **43**, 359–376 (1975).
14. Landini, M. & Monsignori-Fossi, B. C. A loop model of active coronal regions. *Astron. Astrophys.* **42**, 213–220 (1975).
15. Hollweg, J. V. in *Solar Wind 5* (NASA CP 2280) 5–21 (NASA, Washington DC, 1983).
16. Roberts, B. in *Hydromagnetics of Sun* (ESA SP-220) 137–145 (ESA, Noordwijk, 1984).
17. Heyvaerts, J. & Priest, E. R. Coronal heating by phase-mixed shear Alfven waves. *Astron. Astrophys.* **117**, 220–234 (1983).
18. Hood, A. W., Ireland, J. & Priest, E. R. Heating of coronal holes by phase mixing. *Astron. Astrophys.* **318**, 957–961 (1997).
19. Goedbloed, J. P. *Lecture Notes on Ideal MHD* (Rijnhuizen Report) 83–145 (1983).
20. Goossens, M. in *Advances in Solar System MHD* (eds Priest, E. R., Hood, A. W.) 137–172 (Cambridge Univ. Press, 1991).
21. Davila, J. M. Heating of the solar corona by resonant absorption of Alfvèn waves. *Astrophys. J.* **317**, 514–521 (1987).
22. Tucker, W. H. Heating of solar active regions by magnetic energy dissipation: the steady state case. *Astrophys. J.* **186**, 285–289 (1975).
23. Levine, R. Evidence for opposed currents in active-region loops. *Solar Phys.* **46**, 159–170 (1976).
24. Galeev, A. A., Rosner, R., Serio, S. & Vaiana, G. S. Dynamics of coronal structures: magnetic field related heating and loop energy balance. *Astrophys. J.* **243**, 301–308 (1981).
25. Parker, E. N. *Spontaneous Current Sheets in Magnetic Fields* (Oxford Univ. Press, 1994).
26. Berger, M. A. in *Advances in Solar System MHD* (eds Priest, E. R. & Hood, A. W.) 241–256 (Cambridge Univ. Press, 1991).
27. Heyvaerts, J. & Priest, E. R. A self-consistent turbulent model for coronal heating. *Astrophys. J.* **390**, 297–308 (1993).
28. Einaudi, G., Velli, M., Politano, H. & Pouquet, A. Energy release in a turbulent corona. *Astrophys. J.* **457**, L113–L116 (1996).
29. Hendrix, D. L., Van Hoven, G., Mikic, Z. & Schnack, D. D. The viability of Ohmic dissipation as a coronal heating source. *Astrophys. J.* **470**, 1192–1197 (1996).
30. Galsgaard, K. & Nordlund, A. Heating and activity of the solar corona 1. Boundary shearing of an initially homogeneous magnetic field. *J. Geophys. Res.* **101**, 13445–13460 (1996).

Acknowledgements. We are most grateful for financial support from the UK Particle Physics and Astronomy Research Council and to S. T. Buckland for helpful suggestions. Part of the work was carried out while one of us (J.L.C.) was a visiting professor at the Institute for Space and Astronautical Science (ISAS) of Japan. C.R.F. was supported by a Research Studentship from PPARC. NASA supported the work of L.W.A. The Yohkoh mission and its continued operation are projects of ISAS in Japan.

Correspondence and requests for materials should be addressed to E.R.P. (e-mail: eric@dcs.st-and.ac.uk).

Chemical processing in the coma as the source of cometary HNC

William M. Irvine*, Edwin A. Bergin†, James E. Dickens*, David Jewitt‡, Amy J. Lovell*, Henry E. Matthews§‖, F. Peter Schloerb* & Matthew Senay*

** Five College Radio Astronomy Observatory, 619 LGRC, University of Massachusetts, Amherst, Massachusetts 01003, USA*
† Smithsonian Astrophysical Observatory, MS-66, 60 Garden Street, Cambridge, Massachusetts 02138-1596, USA
‡ Institute for Astronomy, University of Hawaii, 2680 Woodlawn Drive, Honolulu, Hawaii 96822, USA
§ Herzberg Institute of Astrophysics, National Research Council of Canada, Ottawa, Ontario K1A 0R6, Canada
‖ Joint Astronomy Centre, 660 N. A'ohoku Place, University Park, Hilo, Hawaii 96720, USA

The discovery of hydrogen isocyanide (HNC) in comet Hyakutake with an abundance (relative to hydrogen cyanide, HCN) similar to that seen in dense interstellar clouds raised the possibility that these molecules might be surviving interstellar material[1]. The preservation of material from the Sun's parent molecular cloud would provide important constraints on the processes that took place in the protostellar nebula. But another possibility is that

HNC is produced by photochemical processes in the coma, which means that its abundance could not be used as a direct constraint on conditions in the early Solar System. Here we show that the HNC/HCN ratio determined for comet Hale–Bopp varied with heliocentric distance in a way that matches the predictions of models of gas-phase chemical production of HNC in the coma, but cannot be explained if the HNC molecules were coming from the comet's nucleus. We conclude that HNC forms mainly by chemical reactions in the coma, and that such reactions need to be considered when attempting to deduce the composition of the nucleus from observations of the coma.

The $J = 4$–3 pure rotational transitions[2,3] of both HCN and HNC were observed in comet Hale–Bopp (C/1995 O1) at the James Clerk Maxwell Telescope (Fig. 1). The lines of both species were either observed simultaneously or within, at most, one hour of each other at approximately equal zenith angles. Such timing is very important, as intra-day variations in at least the HCN emission arise as the comet rotates and undergoes outbursts[4,5].

Table 1 gives the observed intensities integrated over the line frequencies, I(HCN) and I(HNC). The ratio, $R_{thin} = I(HNC)/I(HCN)$, will closely approximate the ratio of column densities (average number of molecules per cm^2 in the telescope beam), apart from effects of optical depth (Table 1). In fact, R_{thin} will be an upper limit to the true ratio of column densities, as the HCN lines are sufficiently strong to ensure that we need to consider their opacity. It is clear that R_{thin} increases strongly as the comet approaches the Sun. Such an increase is also apparent in the results published by Biver *et al.*[6,7], who, however, do not discuss opacity effects.

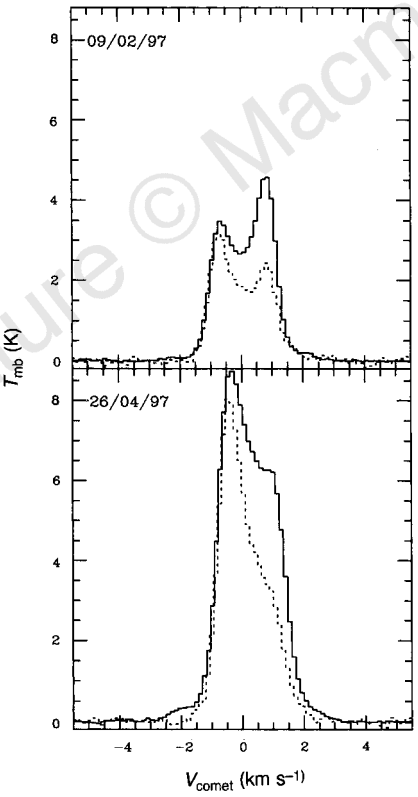

Figure 1 The J(4–3) lines of HNC (dashed lines) and HCN (solid lines, spectra multiplied by 0.25) for comet Hale–Bopp. Observations were made with the James Clerk Maxwell Telescope on the indicated dates. The velocity scale is with respect to the nucleus, and the intensity scale is main beam brightness temperature. The double-peaked profiles that are often observed are indicative of an expanding and resolved shell of gas, such as those seen around many evolved stars[24].

A critical question is whether the heliocentric variation in R_{thin} might be solely an effect of the increasing opacity of the HCN line, as the comet approaches the Sun and outgassing increases. Determining the optical depth of the HCN emission is difficult, as it involves assumptions about the distribution and kinematics of the coma gas, and the excitation of HCN. There are, in principle, two mitigating factors in such determinations: the $J = 4$–3 transition of HCN has two weak hyperfine components (each ~2% of the total line strength) that are partially resolved from the three strongest, overlapping hyperfine components; also, we have some observations of the rarer isotopomer, H^{13}CN.

An estimate of the possible saturation was obtained by assuming that the observed HCN emission originated in a homogeneous slab of gas, so that the excitation temperature (T_x) was constant in the observed region and the line width was the result of random mass motions on a scale smaller than the beam of our telescope. In the present case, this approach should generally overestimate possible opacity effects, because in a more realistic expanding coma the systematic velocity gradients will make it easier for photons emitted in the interior of the coma to escape. The results show that the HCN line has at most a moderate opacity, with maximum values $1 < \tau < 2$, consistent with the clearly optically thin profiles for the $J = 1$–0 transition[8] and with the relative intensities of the HCN and H^{13}CN lines when both were observed. A sample fit is shown in Fig. 2.

Correcting the optically thin abundance ratio for partial saturation of the HCN lines, and assuming that the HNC lines are optically thin, produces an approximate lower bound on the column density ratio: $R_{thick} = a(\tau)R_{thin}$, where $a(\tau) = (1 - e^{-\tau})/\tau$, τ is the optical depth for the HCN line, and we have adopted those fit parameters that produce the largest values of τ for observations on a given date.

The fundamental question we wish to resolve is whether HCN and HNC are present primarily as ices in the cometary nucleus, rather than being produced in the coma. Laboratory experiments show that, once water ice begins to sublime rapidly (heliocentric distance $r \leqslant 4$ AU), the sublimation of trace nuclear constituents is controlled by that of H_2O (ref. 9); this is consistent with the constant relative production rates of HCN and H_2O as a function of r

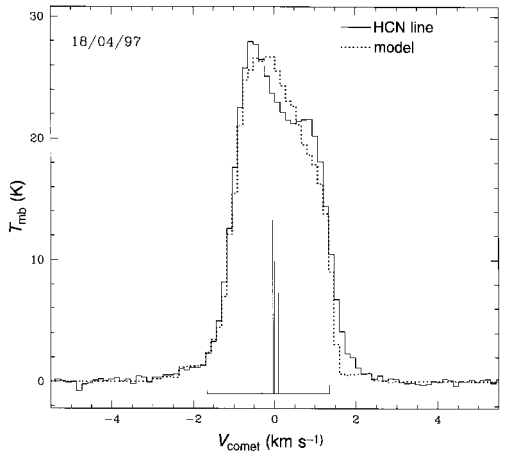

Figure 2 Comparison of an observed $J = 4$–3 HCN line (solid line; for indicated date) with a radiative transfer model (dashed line). Here we used the $J = 1$–0, $F = 2$–1, line profile to estimate the optical depth of the $J = 4$–3 line. We note hyperfine components of $J = 4$–3 line at positions indicated by vertical markers; height of markers shows relative line strength. We solved iteratively for the values of linewidth ΔV and line centre optical depth (τ) which best matched the total observed HCN line shape, including the weak hyperfine components. In our solutions the deduced values of τ were not very dependent on the normalized line profile or on whether or not the line excitation temperature was fixed or was a free parameter (a more complete analysis will be given elsewhere)[13].

Table 1 Observations and abundance ratios for HCN and HNC

Date (dd/mm/yy)	r (AU)	Δ (AU)	I(HCN) (K km s^{-1})	I(HNC) (K km s^{-1})	τ_{max}	R_{thin} (%)	R_{thick} (%)
14/07/96	3.779	2.798	0.79 (0.02)	<0.09	–	<11.4	–
06/09/96	3.177	2.850	1.65 (0.02)	<0.02	–	<1.2	–
30/11/96	2.157	2.933	3.23 (0.03)	0.22 (0.02)	0.19 (0.09)	6.8	6.2
18/01/97	1.539	2.273	10.78 (0.03)	1.48 (0.05)	0.30 (0.12)	13.7	11.9
19/01/97	1.527	2.255	10.96 (0.06)	1.44 (0.09)	0.31 (0.11)	13.1	11.3
08/02/97	1.286	1.866	21.93 (0.05)	3.82 (0.06)	0.52 (0.13)	17.4	13.6
09/02/97	1.274	1.846	21.12 (0.02)	3.55 (0.02)	0.50 (0.11)	16.8	13.2
09/02/97*	1.274	1.846	7.62 (0.02)	1.45 (0.03)	0.16 (0.05)	19.0	17.6
16/02/97	1.196	1.711	28.52 (0.03)	4.72 (0.02)	1.22 (0.13)	16.6	9.6
09/03/97	1.003	1.387	31.91 (0.02)	6.46 (0.03)	–	20.2	–
15/03/97	0.964	1.338	49.75 (0.12)	11.01 (0.16)	0.95 (0.21)	22.1	14.3
22/03/97	0.932	1.315	79.20 (0.11)	20.96 (0.18)	1.81 (0.31)	26.5	12.2
18/04/97	0.962	1.555	37.30 (0.07)	8.30 (0.08)	0.72 (0.10)	22.3	15.9
26/04/97	1.015	1.685	43.77 (0.03)	7.52 (0.02)	0.91 (0.13)	17.2	11.3
08/06/97	1.473	2.369	22.17 (0.05)	3.06 (0.05)	–	13.8	–
20/06/97	1.623	2.517	9.64 (0.02)	0.78 (0.02)	0.53 (0.11)	8.1	6.3
14/07/97	1.927	2.747	6.85 (0.03)	0.59 (0.02)	0.13 (0.03)	8.6	8.0
29/08/97	2.500	2.996	2.88 (0.03)	<0.05	–	<1.7	–
30/08/97	2.512	2.999	2.52 (0.02)	<0.05	–	<2.0	–

Date (dd/mm/yy)	r (AU)	Δ (AU)	I(H^{13}CN) (K km s^{-1})
09/02/97	1.274	1.846	0.29 (0.02)
16/02/97	1.196	1.711	0.55 (0.01)
22/03/97	0.932	1.315	1.21 (0.03)
26/04/97	1.015	1.685	0.69 (0.02)

Shown are the integrated intensities (I) for the $J = 4$–3 transitions of HCN and HNC in comet Hale–Bopp, uncorrected for beam efficiency, as a function of heliocentric distance r and geocentric distance Δ; τ_{max} is the maximum value of line-centre optical depth for the HCN line found from fitting the hyperfine structure; R_{thin} and R_{thick} are upper and lower limits, respectively, to the HNC/HCN column density ratios (see text). Detailed observing and calculation procedures will be described elsewhere[13]. In deriving abundances from the observed spectra, we must consider the relative excitation of the $J = 4$ levels of HCN and HNC and the possibility that the stronger HCN line may be partially saturated. With our 14-arcsec (FWHP, or full width half power) beam (corresponding to 10,000 Δ km at the comet) we are observing the inner coma, where the excitation of both HCN and HNC should be dominated by collisions rather than by radiative excitation[20], since the collision-dominated region of the coma is probably a few times 10,000 km in radius[21] even at $r \approx 2$ AU for such an active comet (the gas production rate at that distance[5] was $\sim 10^{30}$ s^{-1}). Then, because the relevant molecular parameters (rotational constant, and hence transition frequency, and electric dipole moment) of HNC and HCN are very nearly equal, their excitation and hence their population distribution over accessible energy levels will be nearly equal, as in dense interstellar clouds[22,23]. In consequence, the ratio of integrated line intensities I(HNC)/I(HCN) will closely approximate the ratio of column densities, apart from effects of optical depth.
* Offset from the nucleus by right ascension 10″, declination 10″.

observed for comet Hale–Bopp[6]. Thus, if HNC and HCN were primarily parent molecules present in the nucleus, their production into the gas phase would vary together, so that the abundance ratio R would not depend on r.

The limits that we have obtained for the variation of R with r are shown in Fig. 3 and listed in Table 1. Even when the varying optical depth of the HCN line is taken into account, the HNC/HCN ratio clearly increases with decreasing heliocentric distance. We conclude that HNC is primarily produced by processes dependent on the strength of the solar radiation field, including the gas production rate. Moreover, the data for $r > 2$ AU, when both the HCN and HNC lines should be optically thin, indicate that any intrinsic HNC/HCN ratio in the nuclear ices of comet Hale–Bopp is less than $\sim$0.02 (3σ).

Among the processes which might produce HNC as the comet approaches the Sun, the most plausible are photodissociation of a heavier ('parent') molecule, evaporation or sputtering from organic ('CHON') grains in the coma, and gas-phase chemistry in the coma[1].

We have investigated the possibility that HNC is the 'daughter' of an unknown parent by calculating the distribution in the coma of HNC for various assumed parent lifetimes against photodissociation, using a Monte Carlo model to track the location of the HNC molecules[10]. For comet Hale–Bopp, maps of the coma distribution of HCN emission are consistent with a nuclear origin[4,5,8]. If the HCN is subliming directly from the nucleus while the HNC is produced in the coma, their distributions as a function of coma position will differ; the abundance ratio must be obtained by convolving the calculated distribution with the antenna beam for the appropriate date. The calculated results (Fig. 3) show a dependence of the HNC/HCN ratio on heliocentric distance which does not match the observations well, irrespective of the parent lifetime.

In contrast, gas-phase chemistry must be important for a comet as active as Hale–Bopp. Certainly HCO^+, emission from which was mapped for the first time in comet Hale–Bopp[4,11], must be produced in this way. We have investigated this situation with a time-

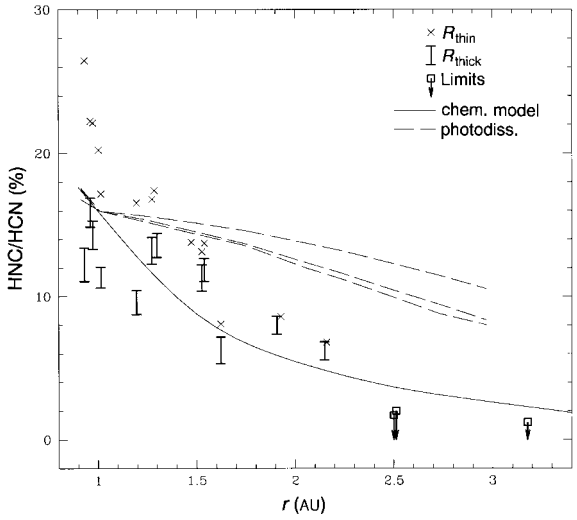

Figure 3 Dependence of the HNC/HCN ratio on heliocentric distance r. R_{thin} is the observed column density ratio assuming that both lines are optically thin, and R_{thick} is the corresponding ratio with the maximum estimate of the HCN opacity correction (error bars show $\pm 1\sigma$ about this value). Open squares are 3σ upper limits. Dashed lines give the calculated[10] HNC/HCN ratio for the case that HCN is subliming from the nucleus while HNC is formed by photodissociation of an unknown nuclear parent which is sufficiently abundant to produce the same value of the ratio as our chemical model at 1 AU. Upper, middle and lower dashed curves are for parent lifetimes in the solar radiation field equal to 0.1, 1.0 and 10 times that of HCN (ref. 25), respectively. The results of our chemical model are shown as a solid line. The model water production rate (molecules s^{-1}) was set equal to $10^{31}\, r^{-1.6}$ (here r is in AU; this value is the approximate rate given in ref. 26); the abundances in the nuclear ices were set to the reported relative production rates at 1.5 AU (that is, when the water ice is subliming rapidly[6,11]), except that the nuclear abundance of HNC was set equal to zero; and the outflow velocity was taken to be 1 km s^{-1}.

dependent interstellar chemical model[12], adapted to the cometary conditions (details will be published elsewhere[13]; see also Fig. 3 legend). We find that HCN undergoes proton transfer from H_3O^+ to produce $HCNH^+$, which can in turn react by proton transfer with H_2CO and NH_3, or by dissociative recombination with electrons to give HNC (and HCN). Dissociative recombination is the most important pathway according to our calculations. Although there are a number of somewhat uncertain parameters in the model, the similar production and destruction pathways for HNC and HCN make the calculated HNC/HCN ratio rather insensitive to most of these parameters. For example, we find that varying the initial (nuclear) abundances of various nitrogen-containing species over a wide range ($0 < N_2 < 0.3$; $0.002 < NH_3 < 0.05$, relative to H_2O) has little effect on the HNC/HCN ratio.

The parameters crucial to the calculated HNC/HCN ratio are the branching ratios for the principal HNC production route, $HCNH^+ + e$. There are no laboratory measurements of these ratios, and the standard values used for interstellar chemistry assume that this dissociative recombination yields HCN:HNC:CN in the ratios 0.25:0.25:0.5 (ref. 14). However, very recent quantum-chemical calculations suggest that the production of HNC should exceed that of HCN and that little CN will be produced[15]. This is consistent with the conclusions from extensive observations of HCN and HNC isotopomers in the interstellar medium, from which the branching ratios are deduced to be[16] HCN:HNC:CN = 0.4:0.6:0. We adopt here the slightly more conservative ratios HCN:HNC:CN = 0.45:0.55:0.

The results of this chemical model are plotted in Fig. 3. The model matches the observations very well, both in terms of the maximum value of the HNC/HCN ratio and in terms of the dependence of this ratio on heliocentric distance r. The nonlinear character of the dependence on r seems to be a result of the multi-stage chemical process which produces HNC and the density-squared dependence of the bimolecular reactions involved.

A source for HNC from the CHON grains[17,18] in the coma might involve multiple processes which could conceivably mimic the observed heliocentric dependence, and can perhaps not be completely ruled out. However, we feel that HNC in Hale–Bopp must be produced in significant measure by gas-phase, ion–molecule chemistry initiated by the photoionization of H_2O. A similar conclusion has been reached with an independent chemical model by Rodgers and Charnley[19], and our chemical model also predicts an abundance and coma distribution of HCO^+ in agreement with the observations[11]. We conclude that HNC is, to our knowledge, the first neutral cometary molecule whose existence in active comets can be ascribed in large part to chemical processes in the coma. As a corollary, it follows that in such comets the effects of chemistry in the coma must be included in deducing the original composition of the nucleus. □

Received 9 October 1997; accepted 30 March 1998.

1. Irvine, W. M. *et al.* Spectroscopic evidence for interstellar ices in comet Hyakutake. *Nature* **383,** 418–420 (1996).
2. Lovas, F. J. Recommended rest frequencies for observed interstellar molecular microwave transitions—1991 revision. *J. Phys. Chem. Ref. Data* **21,** 181–271 (1992).
3. Bockele'e-Morvan, D., Padman, R., Davies, J. K. & Crovisier, J. Observations of submillimeter lines of CH_3OH, HCN, and H_2CO in comet P/Swift-Tuttle with the James Clerk Maxwell Telescope. *Planet. Space Sci.* **42,** 655–662 (1994).
4. Lovell, A. J. *et al.* HCO+ imaging of comet C/1995 O1 Hale-Bopp. *Astrophys. J. Lett.* **497,** L117–L121 (1998).
5. Wink, J. *et al.* Evidence for extended sources and temporal modulations in molecular observations of C/1995 O1 (Hale-Bopp) at the IRAM interferometer. *Earth Moon Planets* Abstr. (in the press).
6. Biver, N. *et al.* Evolution of the outgassing of Comet Hale-Bopp (C/1995 O1) from radio observations. *Science* **275,** 1915–1918 (1997).
7. Biver, N. *et al.* Long-term evolution of the outgassing of comet Hale-Bopp from radio observations. *Earth Moon Planets* (in the press).
8. Irvine, W. M. *et al.* in *The Far Infrared and Submillimetre Universe* (ed. Wilson, A.) 277–280 (SP-401, ESA, Noordwijk Netherlands, 1997).
9. Notesco, G. & Bar-Nun, A. Trapping of methanol, hydrogen cyanide, and *n*-hexane in water ice, above its transformation temperature to the crystalline form. *Icarus* **126,** 336–341 (1997).
10. Tacconi-Garman, L. E., Schloerb, F. P. & Claussen, M. J. High spectral resolution observations and kinematic modeling of the 1667 MHz hyperfine transition of OH in comets Halley (1982i), Giacobini-Zinner (1984e), Hartley-Good (1985l), Thiele (1985m), and Wilson (1986l). *Astrophys. J.* **364,** 672–686 (1990).
11. Lovell, A. J. *et al.* HCO+ ion-molecule chemistry in comet C/1995 O1 Hale-Bopp. *Earth Moon Planets* (in the press).
12. Bergin, E. A. & Langer, W. D. Chemical evolution in pre-protostellar and protostellar cores. *Astrophys. J.* **486,** 316–328 (1997).
13. Irvine, W. H. *et al.* Chemistry in cometary comae. *Faraday Discuss.* **109** (in the press).
14. Herbst, E. What are the products of polyatomic ion-electron dissociative recombination reactions? *Astrophys. J.* **222,** 508–516 (1978).
15. Shiba, Y., Hirano, T., Nagashima, U. & Ishii, K. Potential energy surfaces and branching ratio of the dissociative recombination reaction $HCNH^+ + e^-$: An *ab initio* molecular orbital study. *J. Chem. Phys.* **108,** 698–705 (1998).
16. Hirota, T., Yamamoto, S., Mikami, H. & Ohishi, M. Abundances of HCN and HNC in dark cloud cores. *Astrophys. J.* (in the press).
17. Mumma, M. J., Weissman, P. R. & Stern, S. A. in *Protostars and Planets III* (eds Levy, E. H. & Lunine, J. I.) 1177–1252 (Univ. Arizona Press, Tucson, 1993).
18. Fomenkova, M. in *From Stardust to Planetesimals* (eds Pendleton, Y. J. & Tielens, A. G. G. M.) 415–421 (ASP Conf. Ser.122, Astron. Soc. Pacific, San Francisco, 1997).
19. Rodgers, S. D. & Chamley, S. B. HNC and HCN in comets. *Astrophys. J. Lett.* (in the press).
20. Crovisier, J. Rotational and vibrational synthetic spectra of linear parent molecules in comets. *Astron. Astrophys. Suppl.* **68,** 223–258 (1987).
21. Festou, M. C., Rickman, H. & West, R. M. Comets II. Models, evolution, origin and outlook. *Astron. Astrophys. Rev.* **5,** 37–163 (1993).
22. Goldsmith, P. F., Langer, W. D., Ellder, J., Irvine, W. M. & Kollberg, E. Determination of the HNC to HCN abundance ratio in giant molecular clouds. *Astrophys. J.* **249,** 524–531 (1981).
23. Goldsmith, P. F., Irvine, W. M., Hjalmarson, Å & Ellder, J. Variations in the HCN/HNC abundance ratio in the Orion moelcular cloud. *Astrophys. J.* **310,** 383–391 (1986).
24. Olofsson, H., Johansson, L. E. B., Hjalmarson, Å. & Nguyen-Quang-Rieu High sensitivity molecular line observations of IRC +10216. *Astron. Astrophys.* **107,** 128–144 (1982).
25. Schmidt, H. U., Wegman, R., Huebner, W. F. & Boice, D. C. Cometary gas and plasma flow with detailed chemistry. *Comput. Phys. Commun.* **49,** 17–59 (1988).
26. *Proc. 1st Int. Conf. on Comet Hale-Bopp* (to be published as a special issue of *Earth, Moon, Planets*).

Acknowledgements. We thank B. Marsden and D. Tholen for rapidly providing us with the best available cometary elements, and the staff at the JCMT for their assistance with the observations. This work was partly supported by the NSF and NASA.

Correspondence and requests for materials should be addressed to W.M.I. (e-mail: irvine@fcrao1.phast.umass.edu).

Electronic liquid-crystal phases of a doped Mott insulator

S. A. Kivelson*, E. Fradkin† & V. J. Emery‡

* *Department of Physics, University of California Los Angeles, Los Angeles, California 90095, USA*

† *Department of Physics, University of Illinois, Urbana, Illinois 61801-3080, USA*

‡ *Brookhaven National Laboratory, Upton, New York 11973-5000, USA*

The character of the ground state of an antiferromagnetic insulator is fundamentally altered following addition of even a small amount of charge[1]. The added charge is concentrated into domain walls across which a π phase shift in the spin correlations of the host material is induced. In two dimensions, these domain walls are 'stripes' which can be insulating[2,3] or conducting[4–6]—that is, metallic 'rivers' with their own low-energy degrees of freedom. However, in arrays of one-dimensional metals, which occur in materials such as organic conductors[7], interactions between stripes typically drive a transition to an insulating ordered charge-density-wave (CDW) state at low temperatures. Here it is shown that such a transition is eliminated if the zero-point energy of transverse stripe fluctuations is sufficiently large compared to the CDW coupling between stripes. As a consequence, there should exist electronic quantum liquid-crystal phases, which constitute new states of matter, and which can be either high-temperature superconductors or two-dimensional anisotropic 'metallic' non-Fermi liquids. Neutron scattering and other experiments in the copper oxide superconductor $La_{1.6-x}Nd_{0.4}Sr_xCuO_4$ already provide evidence for the existence of these phases in at least one class of materials.

Classical liquid crystals[8] are phases that are intermediate between a liquid and a solid, and spontaneously break the rotation and/or translation symmetries of free space. The proposed electronic liquid crystals are quantum analogues of these phases in which the ground state is intermediate between a liquid, where quantum fluctuations